Estimated Frequency Domain Model Uncertainties used in Robust Controller Design – A μ-Approach*

Steen Tøffner-Clausen and Palle Andersen

Department of Control Engineering
Aalborg University
DK-9220 Aalborg Ø, Denmark

Jakob Stoustrup and Hans H. Niemann

Mathematical Institute
Technical University of Denmark
DK-2800 Lyngby, Denmark

Abstract

This paper deals with the combination of system identification and robust controller design. Recent results on estimation of frequency domain model uncertainty are utilized in robust analysis and controller design using μ. It is shown how estimated frequency domain uncertainty ellipses may be represented within the general μ-framework using a mixed perturbation set. A methodology for synthesizing optimal mixed perturbation set μ-controllers has been developed. A control design strategy achieving – if possible – robust performance control systems given the uncertainty estimates could then be formulated. The design method was successfully applied to a laboratory centrifugal pump/induction motor configuration resembling a small domestic water supply system.

1 Introduction

The combination of system identification and robust controller design has been the focus of active research during the last couple of years, see e.g. [1] and references therein. However only a very limited number of practical application results have been published.

In this paper we will show how μ-based methods for analyzing the performance and robustness of systems with structured uncertainties may be combined with stochastic embedding methods for estimation of frequency domain model uncertainties. The combination allows for coherent model identification and robust controller design. A design procedure for SISO plants has been developed and has been successfully applied to a domestic water supply test system, including an AC-motor driven centrifugal pump.

The remaining part of the paper has been organized as follows. A short review of the main results from mixed perturbation set μ-theory will be presented in Section 2. In Section 3 a methodology for synthesizing optimal μ-controllers given a mixed perturbation set will be developed. Then the main principles of the stochastic embedding methodology for uncertainty estimation will be reviewed in Section 4. In Section 5 it will be demonstrated how the estimated frequency domain uncertainty ellipses may be expressed in a general μ framework. In Section 6 a general design procedure for SISO-systems will be outlined and finally in Section 7 the design procedure will be applied to a laboratory pump/induction motor configuration.

*This work is supported by the Danish Technical Research Council under grant no. 26-1830.

2 Robust Stability and Performance

The general framework for robustness analysis of linear systems is illustrated in Figure 1. Any linear interconnection of control inputs u, measured outputs y, disturbances d', controlled outputs e', perturbations w and a controller K can be expressed within this framework. For the particular problem addressed in this paper the rearrangement is simple and illustrative. Within the general framework analysis

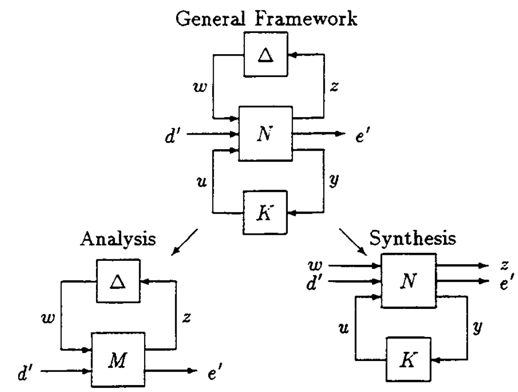

Figure 1: *The general μ framework with emphasis on analysis and synthesis.*

and synthesis constitutes two special cases as illustrated in Figure 1. Conventionally scalings and weights are absorbed into the transfer function M in order to normalize d', e' and Δ to norm 1. For robust analysis the transfer function F_u from d' to e' may be partitioned as a linear fractional transformation:

$$e' = F_u(M, \Delta)d' \quad (1)$$

$$= \left[M_{22} + M_{21}\Delta\left(I - M_{11}\Delta\right)^{-1} M_{12}\right] d' \quad (2)$$

Δ is a member of the bounded subset:

$$\mathbf{B\Delta} = \{\Delta \in \mathbf{\Delta} \,|\, \bar{\sigma}(\Delta) < 1\} \quad (3)$$

where $\bar{\sigma}$ denotes largest singular value and $\mathbf{\Delta}$ is defined by:

$$\mathbf{\Delta} = \left\{\mathrm{diag}\left(\delta_1^r I_{r_1}, \cdots, \delta_{m_r}^r I_{r_{m_r}}, \delta_1^c I_{r_{m_r+1}}, \cdots, \delta_{m_c}^c I_{r_{m_r+m_c}},\right.\right.$$

0-7803-1872-2/94/$4.00 © 1994 IEEE

$\Delta_1,\cdots,\Delta_n)\,\big|\delta_i^r\in\mathbf{R},\delta_i^c\in\mathbf{C},\Delta_j\in\mathbf{C}^{r_{m_r+m_c+j}\times r_{m_r+m_c+j}}\big\}$ (4)

The positive real-valued function μ is then defined by:

$$\mu_{\mathbf{\Delta}}(M)\triangleq\frac{1}{\min\{\bar\sigma(\Delta):\Delta\in\mathbf{\Delta},\det(I-M\Delta)=0\}} \tag{5}$$

unless no $\Delta\in\mathbf{\Delta}$ makes $I-M\Delta$ singular, in which case $\mu_{\mathbf{\Delta}}(M)=0$.

Unfortunately Equation (5) is not suitable for computing μ since the implied optimization problem may have multiple local maxima [2]. However upper and lower bounds for μ may be effectively computed for both complex and mixed perturbations sets. Algorithms for computing these bounds have been documented in several papers, see e.g. [2, 3]. For $M\in\mathbf{C}^{n\times n}$, define β_{min} as:

$$\beta_{min}=\inf_{\beta\in\mathbf{R}_+,G\in\mathbf{G},D\in\mathbf{D}}\Big\{\beta\,\Big|\bar\sigma\Big[\left(I+G^2\right)^{-\frac14}\left(DMD^{-1}-j\beta G\right)\left(I+G^2\right)^{-\frac14}\Big]\le\beta\Big\} \tag{6}$$

then

$$\max_{Q\in\mathbf{Q}}\rho(QM)\le\mu_{\mathbf{\Delta}}(M)\le\beta_{min} \tag{7}$$

Here ρ denotes spectral radius and $\mathbf{Q}$ is the set:

$$\mathbf{Q}=\left\{Q\in\mathbf{\Delta}\,\middle|\delta_i^r\in[-1;1],\delta_i^{c*}\delta_i^c=1,\Delta_j^*\Delta_j=I_{r_{m_r+m_c+j}}\right\} \tag{8}$$

where * denotes complex conjugate and $\mathbf{D}$ is the set of invertible matrices:

$$\mathbf{D}=\Big\{\mathrm{diag}\left(D_1,\cdots,D_{m_r+m_c},d_1I_{r_{m_r+m_c+1}},\cdots,d_nI_{r_m}\right)\,\Big|D_i\in\mathbf{C}^{r_i\times r_i},\det D_i\neq0,d_j\in\mathbf{C},d_j\neq0\Big\} \tag{9}$$

where $r_m=r_{m_r+m_c+n}$. Finally, $\mathbf{G}$ is the set:

$$\mathbf{G}=\{\mathrm{diag}\left(g_1,\cdots,g_{n_r},0_{n_c}\right)|g_i\in\mathbf{R}\} \tag{10}$$

where $n_r=\sum_{i=1}^{m_r}r_i$ and $n_c=n-n_r$.

For purely complex perturbation sets ($G=0$) the above bounds reduce to:

$$\max_{Q\in\mathbf{Q}}\rho(QM)\le\mu_{\mathbf{\Delta}}(M)\le\inf_{D\in\mathbf{D}}\bar\sigma\left(DMD^{-1}\right) \tag{11}$$

with

$$\mathbf{D}=\Big\{\mathrm{diag}\left(D_1,\cdots,D_{m_r+m_c},d_1I_{r_{m_r+m_c+1}},\cdots,d_nI_{r_m}\right)\,\Big|D_i\in\mathbf{C}^{r_i\times r_i},D_i^*=D_i>0,d_j\in\mathbf{R},d_j>0\Big\} \tag{12}$$

In Equation (7) and (11) the lower bound is actually an equality [3] but unfortunately the function $\rho(QM)$ is nonconvex so we cannot guarantee to find the global maximum and hence we only obtain a lower bound for μ.

In this paper the algorithms provided in the *μ-Analysis and Synthesis ToolBox* for use with MATLAB[1] [4] were used for computing μ-bounds.

We now have the following two Theorems for assessing robust stability and robust performance [2]:

[1]MATLAB is a registered trademark of The MathWorks, Inc.

Theorem 1: The controlled system is stable for all $\Delta\in\mathbf{B\Delta}$ iff:

$$\|\mu_{\mathbf{\Delta}}(M_{11})\|_\infty\le1$$

where:

$$\|\mu_{\mathbf{\Delta}}(M_{11})\|_\infty\triangleq\sup_\omega\mu\left(M_{11}\left(e^{j\omega T_s}\right)\right)$$

Theorem 2: Let an $\mathcal{H}_\infty$ performance specification be given on the transfer function from d' to e' — typically a weighted sensitivity specification — of the form:

$$\|F_u(M,\Delta)\|_\infty=\sup_\omega\bar\sigma\left(F_u(M,\Delta)\right)<1$$

Then $F_u(M,\Delta)$ is stable and $\|F_u(M,\Delta)\|_\infty<1\;\;\forall\Delta\in\mathbf{B\Delta}$ iff

$$\|\mu_{\tilde{\mathbf{\Delta}}}(M)\|_\infty\le1$$

where the perturbation set is augmented with a full complex performance block:

$$\tilde{\mathbf{\Delta}}=\left\{\mathrm{diag}\left(\Delta,\Delta_p\right)\middle|\Delta\in\mathbf{\Delta},\Delta_p\in\mathbf{C}^{k\times k},\bar\sigma\left(\Delta_p\right)<1\right\}$$

Theorem 2 is the real payoff for measuring performance in terms of the ∞-norm and bounding model uncertainty in the same manner. Using μ it is then possible to test for both robust stability and robust performance in a nonconservative manner. Indeed, if the uncertainty is modeled exactly by Δ — i.e., if all plants in the norm-bounded set can really occur in practice, then the μ condition for robust performance is necessary and sufficient.

3 μ-Controller Design

For robust synthesis the transfer function F_l from $[w\ d']^T$ to $[z\ e']^T$ may be partioned as the linear fractional transformation:

$$\begin{bmatrix} z\\ e'\end{bmatrix}=F_l(N,K)\begin{bmatrix} w\\ d'\end{bmatrix} \tag{13}$$

$$=\left[N_{11}+N_{12}K\left(I-N_{22}K\right)^{-1}N_{21}\right]\begin{bmatrix} w\\ d'\end{bmatrix} \tag{14}$$

Noticing that $F_l(N,K)=M$ and using Theorem 2 a stabilizing controller K achieves robust performance if and only if for each frequency $\omega\in[0,\infty]$, the structured singular value satisfies:

$$\mu_{\tilde{\mathbf{\Delta}}}\left(F_l(N,K)\left(e^{j\omega T_s}\right)\right)<1 \tag{15}$$

In pursuit of the optimal μ-controller inspired from the upper bound in (7) we will construct the interconnection scheme $\mathcal{P}(z)$ given by:

$$\mathcal{P}(z)=\mathcal{G}_1(z)\left(\mathcal{D}(z)N(z)\mathcal{D}^{-1}(z)-\mathcal{G}_2(z)\right)\mathcal{G}_1(z) \tag{16}$$

where $\mathcal{G}_1(z)$, $\mathcal{G}_2(z)$ and $\mathcal{D}(z)$ are stable transfer function estimates of $(1+G^2)^{-\frac14}$, $j\beta G$ and D respectively (extended properly with trailing ones or zeros) at every frequency ω. We may then pose the optimization problem:

$$\min_{\substack{K(z)\text{ stabilizing}\\ \mathcal{G}_1(z),\mathcal{G}_2(z),\mathcal{D}(z)\text{ stable}}}\left\{\|F_l(\mathcal{P},K)\|_\infty\right\} \tag{17}$$

Unfortunately it is not known how to solve Equation (17) directly. An approximation to μ-synthesis can be made iteratively by a series of minimizations, first over the controller K (holding $\mathcal{G}_1$, $\mathcal{G}_2$ and $\mathcal{D}$ constant), and then over the scaling matrices holding the controller K fixed. This is usually referred to as D-K iteration. D-K iteration works well for complex perturbation sets, since we need only to fit the $\mathcal{D}$-scalings and only in magnitude since any phase in D will be absorbed into the complex perturbation set Δ. However for mixed perturbation sets standard D-K iteration fails since we must fit the $\mathcal{G}$ and $\mathcal{D}$ scalings both in magnitude and phase and because G consists of real elements it will not be possible to generate proper corresponding stable transfer function estimates. We have not been able to find published results within synthesis of mixed perturbation set μ-controllers.

We propose that all the effects of the real perturbations G should be lumped into one multiplicative scaling matrix Γ. The idea is to scale the corresponding complex perturbation set μ-problem to obtain a system with complex perturbations $\tilde{\Delta}_c$ having the same μ-response as the original system with mixed perturbations. Minimizing the μ-value of the scaled system we obtain a (sub-)optimal μ-controller for the mixed perturbation set problem. Consider the interconnection:

$$\mathcal{P}(z) = \Gamma(z)\mathcal{D}(z)N(z)\mathcal{D}^{-1}(z) \quad (18)$$

where $\Gamma(z)$ is a stable transfer function estimate of the frequency dependent scalar γ given by:

$$\gamma(\omega) = \frac{\mu_{\tilde{\Delta}}\left(F_l(N,K)\left(e^{j\omega T_s}\right)\right)}{\mu_{\tilde{\Delta}_c}\left(F_l(N,K)\left(e^{j\omega T_s}\right)\right)} \quad (19)$$

$\tilde{\Delta}_c$ is the corresponding complex perturbation set ($\delta_i^r \in \mathbf{C}$, see Equation (4)). We then pose the optimization problem:

$$\min_{\substack{K(z)\ \text{stabilizing} \\ \Gamma(z),\mathcal{D}(z)\ \text{stable}}} \left\{ \left\| F_l(\Gamma\mathcal{D}N\mathcal{D}^{-1},K)\right\|_\infty \right\} \quad (20)$$

Equation (20) is solved iteratively by a series of minimizations, first over the controller K (holding Γ and $\mathcal{D}$ fixed), and then over the scalings holding the controller K fixed. This can be done since we need only fitting the scaling-matrices in magnitude. We will denote this procedure *modified D-K iteration for mixed perturbation sets.* In (19) upper bounds for μ will be used for computing γ.

4 Estimating the Model Error

A very interesting approach to identification of model uncertainty in the presence of both noise and undermodelling has been manifested through a series of papers by Goodwin & co-workers, see e.g. [5, 6]. The methodology is commonly known as the stochastic embedding approach since stochastic behavior is embedded on the model bias. The main idea of the approach is to impose stochastic behavior not only on the variance error but also on the bias error by assuming that the undermodeling is a random variable with known distribution. Henceforth the true transfer function of the system is assumed to be a stochastic process.

It is furthermore assumed that the true transfer function for the single input single output system may be decomposed as:

$$G_T\left(e^{j\omega T_s}\right) = G\left(e^{j\omega T_s},\theta_0\right) + G_\Delta\left(e^{j\omega T_s}\right) \quad (21)$$

with the following important property:

$$\mathcal{E}\left\{G_T\left(e^{j\omega T_s}\right)\right\} = G\left(e^{j\omega T_s},\theta_0\right) \quad (22)$$

where θ_0 is a vector in the parameter space. Notice that Equations (21) and (22) describe a class of systems from where the true system is just one member. Thus the expectation $\mathcal{E}\{\cdot\}$ in Equation (22) means averaging over different realizations of the undermodeling. Of course, for any given system we will have just one realization. If however, statistical properties of the class of systems defined by (21) and (22) may be determined these properties may be used to evaluate the particular realization in question. Consequently we will estimate the properties of the stochastic process (21) from a single realization, namely the true system.

In [6] an excellent survey of the method is presented assuming white measurement noise and an exponentially decaying undermodelling impulse response. In [7] it is shown how other noise and undermodelling descriptions equally well fit into the framework of the embedding methodology. In this paper we will follow the path outlined in [7] where an ARMA_1 noise description is adopted, frequency domain uncertainty ellipses were computed around the nominal frequency points of the parametric model $G(e^{j\omega T_s},\hat{\theta}_N)$ from a finite set of measured data points.

5 General Framework Formulation

We will now develop a formulation of the estimated frequency domain uncertainty ellipses which fits into the general μ-framework.

The model uncertainty is assumed to be additive, see Equation (21). Unfortunately we cannot directly express frequency domain ellipses using neither a complex nor a mixed perturbation set. Using a mixed perturbation set we may however derive an approximate description of the ellipses. Assume that the additive uncertainty L_a is approximated by the mixed perturbation set:

$$\hat{L}_a = W_c\delta^c + W_r\delta^r \quad (23)$$

where δ^c and δ^r are a complex and a real norm-bounded perturbation:

$$\|\delta^c\| < 1 \qquad -1 < \delta^r < 1 \quad (24)$$

and W_c and W_r are frequency dependent weighting functions. The perturbation set $\hat{L}_a$ then maps into the frequency domain as shown in Figure 2. We will use $\hat{L}_a$ as an approximation of the estimated frequency domain uncertainty ellipses. Consider an ellipse in the complex plane with form matrix P^{-1}:

$$\mathcal{X}^T P_x^{-1}\mathcal{X} = 1 \quad (25)$$

The major and minor principal axes a and b respectively and the major principal axis angle θ is then given by:

$$\begin{aligned} a &= \kappa_1^{-0.5} && (26)\\ b &= \kappa_2^{-0.5} && (27)\\ \theta &= \left\{\theta : \begin{bmatrix}\cos\theta & -\sin\theta \\ \sin\theta & \cos\theta\end{bmatrix} = V\right\} && (28)\end{aligned}$$

where $\{\kappa_1,\kappa_2\}$ is the eigenvalues of the form matrix P^{-1} and V is the corresponding eigenvector matrix. In order to express the estimated uncertainty ellipses the perturbation

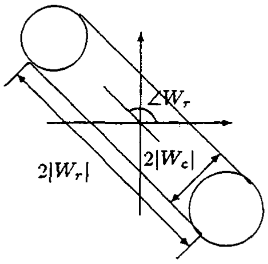

Figure 2: *Frequency domain representation of the perturbation set $\hat{L}_a$.*

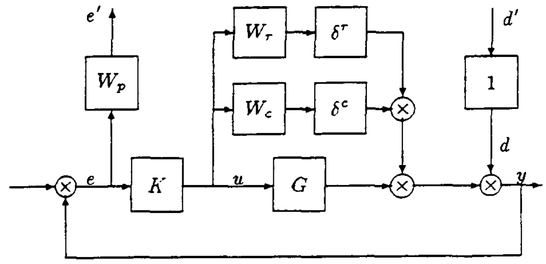

Figure 3: *Nominal system augmented with mixed perturbation set $\hat{L}_a$ and performance specification W_p.*

set weighting functions $W_c(z)$ and $W_r(z)$ consequently must fulfill for every frequency ω:

$$|W_r(e^{j\omega T_s})| \approx a-b \quad \forall\omega \tag{29}$$

$$\angle W_r(e^{j\omega T_s}) \approx \theta \quad \forall\omega \tag{30}$$

$$|W_c(e^{j\omega T_s})| \approx b \quad \forall\omega \tag{31}$$

Least-squares fitting techniques were used to approximate $W_r(z)$ and $W_c(z)$.

6 Design Procedure for SISO Plant

A design procedure for SISO plants may now be formulated. Consider the block diagram in Figure 3 where the plant has been augmented with a mixed perturbation set $\hat{L}_a(z)$ and a performance specification $W_p(z)$ on the error $e(z)$. The transfer function M, see Figure 1, is then given by:

$$M(z) = \begin{bmatrix} W_r\tilde{G}K & W_r\tilde{G}K & W_r\tilde{G}K \\ W_c\tilde{G}K & W_c\tilde{G}K & W_c\tilde{G}K \\ W_p\tilde{G} & W_p\tilde{G} & W_p\tilde{G} \end{bmatrix} \tag{32}$$

where $\tilde{G} = (I+KG)^{-1}$. We propose a design methodology consisting of the following steps:

1. Estimate a parametric model $G(e^{j\omega T_s}, \hat{\theta}_N)$ and frequency domain uncertainty ellipses using system identification and stochastic embedding of the model bias.
2. Fit weighting functions $W_r(e^{j\omega T_s})$ and $W_c(e^{j\omega T_s})$ in order to obtain a mixed perturbation set $\hat{L}_a(e^{j\omega T_s})$ as approximation for the uncertainty ellipses.
3. Specify performance constraints through an additional weighting function $W_p(e^{j\omega T_s})$.
4. Form the interconnection structure $\{\Delta, N, K\}$ given in Figure 1.
5. Synthesize a (sub)-optimal μ-controller using modified *D-K* iteration.

7 Application of the Design Methodology

The outlined design procedure has been applied to a practical example, namely a centrifugal water pump driven by an induction motor. The pump was a typical domestic water supply pump with a capacity of approximately 3 m^3/hr at 2.5 barg. The induction motor was a 840 Watt frequency modulated micro-computer controlled asynchronous type motor. A 3.5 liter rubber membrane buffer tank was placed in the outlet pipe from the pump.

The data acquisition and control of the system were performed using an (A/D, D/A) data acquisition card and a 486 personal computer. Input to the system was the induction motor frequency and the outlet water pressure was recorded as output. The system dynamics was dominated by a low frequency 1st order component with a time constant of approx. 1 sec. The low frequency component originates from the membrane buffer. Furthermore smaller high frequency components originates from the inertia in the induction motor and centrifugal pump.

Identification Procedure

The system was sampled with sampling frequency 50 Hz. The input sequence was a 0.4 Hz fundamental square wave. 500 samples were collected, 300 of which were used to get rid of initial conditions effects. The last 200 samples were used for estimation. A second order Laguerre model:

$$G(z^{-1}) = \frac{\theta_1 z^{-1}}{1+\zeta z^{-1}} + \frac{\theta_2 z^{-1}\left(1-(2+\zeta)z^{-1}\right)}{(1+\zeta z^{-1})^2} \tag{33}$$

was fitted to the data. The Laguerre pole ζ was chosen as 0.96. The least-squares estimate of the parameter vector θ was found as:

$$\hat{\theta} = \begin{bmatrix} 19.2\cdot 10^{-2} & -3.33\cdot 10^{-2} \end{bmatrix}^T \tag{34}$$

Frequency domain uncertainty ellipses were estimated using the stochastic embedding approach. A 90% confidence interval was chosen and the corresponding uncertainty ellipses were used in fitting the weighting functions $W_c(z)$ and $W_r(z)$ as described in Section 5. In Figure 4 the estimated uncertainty ellipses are compared with the corresponding frequency domain representation of $\hat{L}_a(z)$. Also shown are the nominal model and a frequency response estimate measured on the pump using sinosoidal inputs. Notice that the model error estimate gives a fair description of the difference between the model and the measured frequency response. It is seen that $\hat{L}_a(z)$ gives an reasonable description of the estimated model uncertainty.

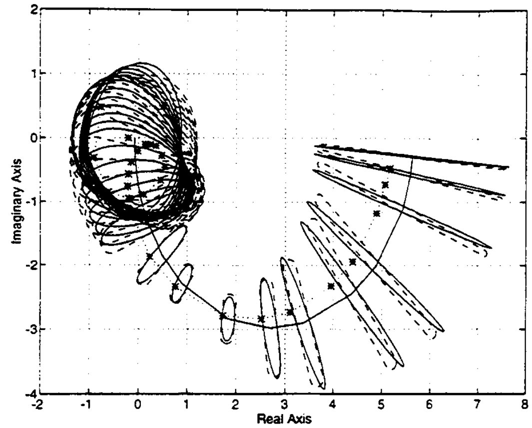

Figure 4: *Comparison of estimated uncertainty ellipses (solid) and $\hat{L}_a(z)$ (dashed). Also shown are the nominal model $G(e^{j\omega T_s}, \hat{\theta}_N)$ (solid) and a frequency response estimate based on pump measurements (∗).*

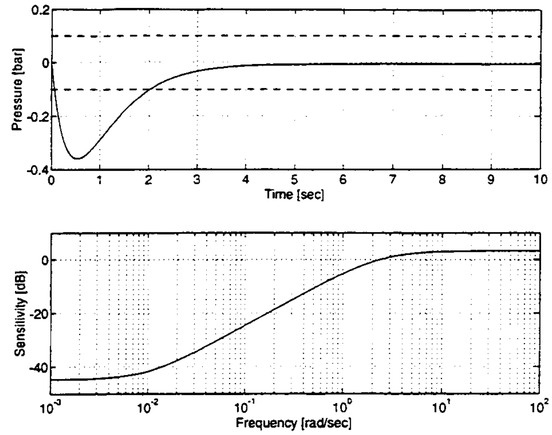

Figure 5: *Time domain response $p_{step}(t)$ (upper) corresponding to the chosen performance specification $S_p(z)$ (lower).*

Performance Specification

Before synthesizing the controller a performance specification must be made. There exists generally no explicit formalisms for obtaining such specifications. In this paper we have used time domain demands on the pump pressure response towards sudden changes in water flow Q, to formulate a maximum sensitivity bound. A standard step of $\Delta Q = 2/3 \text{ m}^3/\text{h}$ was used as the performance measure. The time domain demands on the outlet pressure $p(t)$ given a standard step on $\Delta Q(t)$ were formulated as[2]:

- maximum transient error: 0.4 bar,
- max 0.1 bar settling time: 2 sec,
- max stationary error: 0.1 bar.

It was observed that step disturbances on the flow ΔQ acted approximately through a 1st order system to d. For a standard step $\Delta Q(s) = K_s s^{-1}$ we then have[3]:

$$d_{step}(s) = \frac{K}{s+\tau^{-1}} \cdot \frac{K_s}{s} \tag{35}$$

where K and τ are the gain and time constant of the 1st order filter respectively. $\tilde{K} = KK_s$ and τ were measured on the pump set-up as $\tilde{K} = 1.3 \text{ bar}/(\text{m}^3/\text{h})$ and $\tau = 0.75$ sec. Given a sensitivity specification $S(s) = p(s)/d(s)$ the corresponding time domain response $p_{step}(t)$ may then be computed. We will then use the heuristic assumption that our time demands will be fulfilled for a given compensated system having a sensitivity which falls below the specification for all frequencies. This is probably not guarantied to be true for all systems, but works well in practice.

[2] These demands originates in design goals from a major danish pump producer.

[3] In order to facilitate things we will carry out the derivation for a continuous-time system and simply transform the results to discrete-time.

In this paper a 1st order discrete-time sensitivity specification was chosen:

$$S_p(z) = \frac{1.413z - 1.413}{z - 0.951} \tag{36}$$

As seen in Figure 5 the corresponding time domain response $p_{step}(t)$ fulfill the stated demands.
The $\mathcal{H}_\infty$ performance specification, see Theorem 2, puts a unity bound on the transfer function from d' to e'. Letting $d' = d$ and $e' = W_p e$ we have the performance specification:

$$\frac{e(z)}{d(z)} \le S_p(z) \Rightarrow W_p(z) = S_p^{-1}(z) \tag{37}$$

μ-Synthesis

The first step in synthesizing an optimal μ-controller is to design a optimal $\mathcal{H}_\infty$-controller for the 'nominal' system $N(z)$. We have again used the algorithms provided in [4] for computing the optimal $\mathcal{H}_\infty$-controller. The second step is then to compute upper and lower bounds for $\mu_{\tilde{\Delta}}(M(e^{j\omega T_s}))$. $\tilde{\Delta}$ is for this specific problem given as:

$$\tilde{\Delta} = \left\{ \begin{bmatrix} \delta^r & 0 & 0 \\ 0 & \delta^c & 0 \\ 0 & 0 & \delta^p \end{bmatrix} \middle| \delta^r \in \mathbf{R}, \{\delta^c, \delta^p\} \in \mathbf{C} \right\} \tag{38}$$

In the upper plot of Figure 6 upper and lower bound for $\mu_{\tilde{\Delta}}(M(e^{j\omega T_s}))$ (solid) together with $\bar{\sigma}(M(e^{j\omega T_s}))$ (dashed) are plotted versus frequency ω. Note that the upper and lower bound for μ virtually coincides. We immediately notice that the controlled system does not have robust performance since $\|\mu_{\tilde{\Delta}}(M)\|_\infty \ge 1$. Also notice that the $\mathcal{H}_\infty$-norm $\|(M(e^{j\omega T_s})\|_\infty$ is much larger than the μ-norm since the uncertainty structure cannot be incorporated into the $\mathcal{H}_\infty$-design. In order to improve system performance modified D-K iteration as outlined in Section 3 were applied by performing the iteration:

1. Fit the D-scalings from the complex perturbation set μ upper bound and the ratio γ with stable minimum phase transfer functions $\mathcal{D}(z)$ and $\Gamma(z)$ - the D-iteration step.

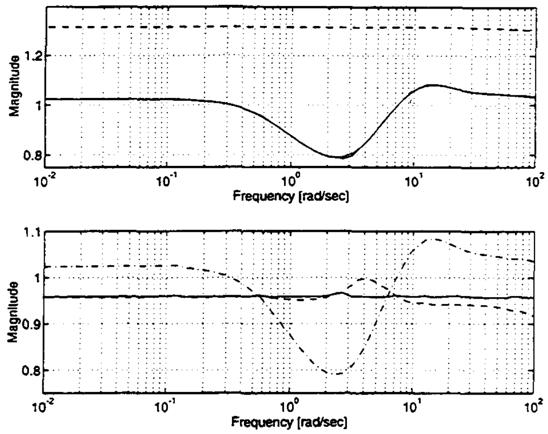

Figure 6: *Results from $\mathcal{H}_\infty$ design (upper) and from modified D-K iteration (lower).*

2. Design an optimal $\mathcal{H}_\infty$-controller $K(z)$ for the augmented system $\Gamma\mathcal{D}^{-1}N\mathcal{D}$ - the K-iteration step.

3. Repeat step 1 and 2 until no further improvement in $\left\|\mu_{\tilde{\Delta}}\left(F_l(N,K)\left(e^{j\omega T_s}\right)\right)\right\|_\infty$ can be obtained.

4. Applying model reduction methods, reduce the order of the controller K as much as possible.

The results of the iteration is displayed in the lower plot of Figure 6. Here the upper bound on μ for the $\mathcal{H}_\infty$ design (dash-dotted) and for the first (dashed) and fourth (solid) *D-K* iteration are shown. Notice how rapidly the *D-K* iteration converges. Only little improvement is obtained after the second iteration. $\left\|\mu_{\tilde{\Delta}}\left(F_l(N,K)(e^{j\omega T_s})\right)\right\|_\infty$ for each iteration is given in Table 1.

Table 1: $\left\|\mu_{\tilde{\Delta}}\left(F_l(N,K)(e^{j\omega T_s})\right)\right\|_\infty$ *for each $D-K$ iteration and for the reduced final controller K_6.*

	$\left\|\mu_{\tilde{\Delta}}\left(F_l(N,K)\left(e^{j\omega T_s}\right)\right)\right\|_\infty$
$\mathcal{H}_\infty$ cont.	1.08
$D-K$ no. 1	1.00
$D-K$ no. 2	0.972
$D-K$ no. 3	0.967
$D-K$ no. 4	0.966
K_6	0.970

The final controller K had 52 states, but was reduced to 6 states with only little degradation in performance, see Table 1.

Test Results

The sixth order controller K_6 was implemented in the laboratory experimental set-up. In order to evaluate controller performance 2 tests were performed. First the system response to a standard flowstep $\Delta Q = 0.67$ m^3/hr was obtained, see upper plot in Figure 7. As seen the disturbance

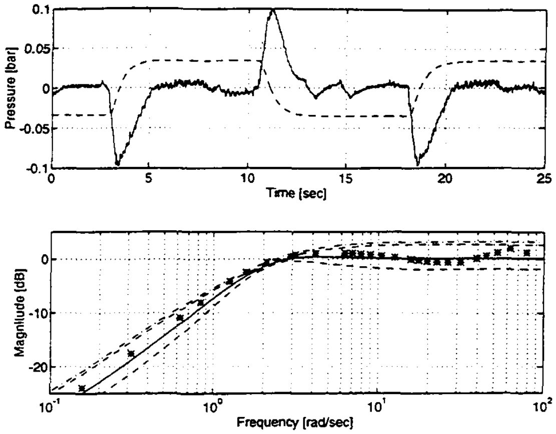

Figure 7: *Test results. In the upper plot the pressure response (solid) to flow steps ΔQ (dashed) is shown. Below the nominal sensitivity (solid) with error bounds (dashed) are compared with the performance specification (dash-dotted) and with measured sensitivity points (*).*

rejection of the controlled system easily complies with the stated demands, see Figure 5.

In order to further investigate system performance a sensitivity measure was made, see lower plot in Figure 7. It is seen that the sensitivity measurements are virtually within the computed error. The error bounds comply very nicely with the performance specification. This is due to the fact that the mixed perturbation set μ response was "squeezed" during the design iteration procedure.

References

[1] J. Baillieul, editor, *IEEE Transactions on Automatic Control*, vol. 37, No. 7, IEEE Control Systems Society, July 1992.

[2] John Doyle and Andrew Packard, *Proc. American Control Conference*, pp. 2147–2152, Minneapolis, MN, 1987.

[3] Peter M. Young, Matthew P. Newlin, and John C. Doyle, *Proc. 30th Conference on Decision and Control*, pp. 1251–1256, Brighton, England, December 1991. IEEE.

[4] Gary J. Balas, John C. Doyle, Keith Glover, Andy Packard, and Roy Smith, *μ-Analysis and Synthesis Toolbox*, The MathWorks Inc., Natick, Mass., USA, First edition, July 1993.

[5] Graham C. Goodwin and Mario E. Salgado, *Int. Journal of Adaptive Control and Signal Processing*, vol. 3, pp. 333–356, 1989.

[6] Graham C. Goodwin, Michel Gevers, and Brett Ninness, *IEEE Transactions on Automatic Control*, vol. 37, pp. 913–928, July 1992.

[7] Palle Andersen and Steen Tøffner-Clausen, "Estimation of frequency domain model uncertainties with application to robust controller design", *in Proc. SYSID'94*, Copenhagen, July 1994.